BIOCAMPATIBLE PHOTO-CORM BIS-(2-HYDROXYNAPHTH-1-YL)CYCLOPROPENONE

by

ROHAN BHAVSAR

(Under the Direction of Vladimir Popik)

ABSTRACT

Carbon monoxide in the last two decades has garnered an increase in interest for its therapeutical effects when applied at a controlled dosage. Some notable effects include anti-inflammation, anti-apoptosis, and anti-oxidation. Presented here is a CO-releasing molecule (CORM), known as bis-(2-hydroxynaphth-1-yl)cyclopropenone, which has the ability to control CO release with duration or intensity of light irradiation, otherwise known as a Photo-CORM. Exposure to light, ideally between the wavelengths of 300 – 420nm, targets the photochemically reactive cyclopropenone ring which induces the release of CO. Quantum yield and fluorescent quantum yield data is then obtained from this interaction which allows the ability to trace the conversion of the release of CO through either UV spectroscopy or measuring the fluorescence emission from the acetylene product. The release of CO is measured using a myoglobin assay, due to the high affinity of the heme-functional groups in myoglobin towards CO, coupled with UV-Vis Spectroscopy. In addition, the effects of CO release towards CT26 colon cancer cells were confirmed via MTT analysis.

INDEX WORDS: CO-releasing molecules, Photo-CORM, myoglobin, UV-Vis Spectroscopy, CT26 cells, MTT Analysis

AN ANALYSIS OF PHOTO-CORM DHNCP

by

ROHAN BHAVSAR

BS, University of Georgia, 2020

A Thesis Submitted to the Graduate Faculty of The University of Georgia in Partial Fulfillment of the Requirements for the Degree

MASTER OF SCIENCE

ATHENS, GEORGIA

2023

AN ANALYSIS OF PHOTO-CORM DHNCP

by

ROHAN BHAVSAR

Major Professor:	Vladimir V. Popik
Committee:	Jin Xie
	Christopher Newton

Electronic Version Approved:

Ron Walcott
Vice Provost for Graduate Education and Dean of the Graduate School
The University of Georgia
May 2023

ACKNOWLEDGEMENTS

I would like to firstly thank my PI Dr. Popik. Since joining his lab in undergrad and now 3 years into graduate school, he has taught me a lot, both in my educational life and personal life. He has been very supportive throughout my time in graduate school, especially during the hard times, which I can't be more thankful for. I would also like to thank all previous and current lab mates for all their help and guidance throughout my time in graduate school. I would also like to thank my committee members, Dr. Xie and Dr. Newton for their guidance and allowing me to learn to become a better scientist. Lastly, I would like to thank Fangchao Jiang, Wei Yang and Zhizi Feng from the Xie lab for their assistance with this project.

TABLE OF CONTENTS

Page

LIST OF TABLES

Page

LIST OF FIGURES

Page

CHAPTER 1

Development of Cancer Therapies and Literature Review

1.1 Introduction

Cancer is a disease in which abnormal or damaged cells grow and multiply uncontrollably and spread to the other parts of the body. As these cells are growing, they can form lumps of tissues known as tumors. The tumors, however, aren't always innately cancerous as they can also be benign, yet when a cancerous tumor is present it can spread throughout the body forming more new tumors. This process is known as metastasis. What causes this phenomenon to occur and what encourages the rapid growth and spread of these abnormal cells? Due to cancer being a genetic disease, the development of cancer to occur can be due to a variety of causes includes: error in cell division, DNA damage due to environmental factors and inheriting cancer genes from parents.[1] After this developmental phase of these cancer cells and once a tumor is formed, the cells can travel through the lymphatic system and/or bloodstream of the body to other parts of the body. If the new location the cells travel to show favorable conditions, i.e. new blood supply, then a new tumor can begin to grow and the process then repeats itself.[2] As this process is occurring, the body targeted by this occurrence can face symptoms such as: fatigue, swelling or lumps on the body, changes to the skin and unusual bleeding or bruising to just name a few as there are a plethora of symptoms associated with the different types of cancers.[3] To combat this disease, various types of cancer therapy

treatments are currently being used as well as constant studies and improvements are being done and made to further treat this disease.

1.2 Cancer Therapy

In 1895 a researcher by the name of Wilhelm Conrad Röntgen had reported the discovery of X-rays after studying this new type of radiation to be able to go through thick screens.[5] Another researcher by the name of Marie Curie expanded on this new discovery to further contribute to the development of radiotherapy, thus leading to the use of radiation to treat tumors. As technology began to see improvements throughout the 20th century, so did the development of cancer therapy. By 1960, the linac or linear accelerator, which allows charged particles to propel through a vacuum, had been developed and a group of scientists by the names of Edward Ginzton and Henry Kaplan used this newfound technology to aid in what was known as rotational linac radiotherapy. This type of radiotherapy worked by concentrating X-rays, using a linac, to more deeply penetrate the body while limiting the harmful effects to the skin of contact.[4] Technological advances at this point have escalated as by the late 20th century modern computer have been developed. This enabled greater advancements in cancer treatment such as the ability to perform three-dimensional X-ray therapy through process such as intensity-modulated radiation therapy (IMRT), where small photons or proton beams of varying intensities irradiate a tumor[6], and computed tomography (CT) scans which is an imaging procedure in which X-rays and computer technology are able to show detailed images of any part of the body (i.e bones, muscles, fat, organs and blood vessels).[7] Present day cancer therapy has seen a great emergence in various treatments, for example, chemotherapy, hormone therapy, hyperthermia, immunotherapy, photodynamic therapy, radiation therapy and stem cell transplants just to name a few. The three treatments that will be further

discussed from here on out are chemotherapy, radiation therapy and photodynamic therapy.

1.3 Chemotherapy

Chemotherapy is a cancer treatment in which drugs are used to kill cancer cells by stopping or slowing the growth of the cancer cells.[8] Once administered to the patient, the drug circulates throughout the bloodstream of the body, targeting cells undergoing cell division. The is to prevent cancer cells from growing and amassing into tumors as these cells divide much more often than normal cells; however, this treatment is not selective towards cancer cells meaning any other cells will also be affected. Despite this outcome, chemotherapy is still widely used in modern cancer treatment as the probability of non-cancer cells to be targeted is low due to cells that are not undergoing division are less likely to be damaged by this treatment.[8-9]

1.4 Radiation Therapy

Radiation therapy is a form a cancer treatment in which high doses of radiation are used to kill or slow the growth of cancer cells by damaging their DNA.[10] When referring to radiation, this does not specifically mean X-rays but a variety of forms of radiation including: radio waves, microwaves, gamma rays and even electrons, protons and neutrons. These forms of radiations can be split into two groups: ionizing radiation and non-ionizing radiation. Ionizing radiation is further split into two major groups which are photon radiation (i.e. X-rays and gamma rays) and particle radiation (i.e. electrons, protons, neutrons and carbon ions). Overall, these radiations input a large amount of energy and can penetrate deeply into tissues. Non-ionizing radiations (i.e. radio waves, microwaves and visible light waves) do not have as much energy as the latter forms of

radiations and are not able to remove electrons from atoms and molecules, thus giving the name non-ionizing radiation. These types of radiations are of no use for radiation therapy as the main purpose of applying radiation is to induce the removal of electrons from surrounding atoms and molecules in the cells of the tissues, thus resulting in the killing of the cancer cells, or stopping the growth of the cancer cell through changing its genes.[10-11] The most common form of administering radiation therapy is through external beam radiation which uses photon beams to irradiate a specific location of the body where the cancer cells are present via the use of a medical linear accelerator.[12] Radiation therapy's selective nature has displayed why this process is still a prominent treatment in modern times even since its first successful case back in 1898.

1.5 Photodynamic Therapy

Another form of cancer treatment that is seeing more interest is photodynamic therapy. This treatment uses a drug that is activated by light to damage or kill the cancer cell, otherwise, known as a photosensitizer.[12] Upon the absorption of light, the photosensitizer molecule is excited to a higher energy orbital. The molecule can undergo a process known as "intersystem crossing" in which the opposite spins of the electrons for the excited singlet state molecule become parallel, resulting in the molecule to be in an excited triplet state. This excited triplet state molecule may undergo an electron transfer reaction which results in the eventually formation of reactive oxygen species (ROS) which are responsible for the damaging of cancer cells. This does not mean that light activation of drugs to combat disease is a new practice, on the contrary, modern phototherapy has been studied and practiced since the start of the 20th century.[13] First accounts of modern phototherapy was seen as early as 1900 in which the first cell death

induced by a photochemical reaction was reported by a medical student named Oscar Raab who worked under Professor Herman von Tappeiner.[13-14] A few years later, von Tappeiner and a dermatologist by the name of Jesionek conducted the first medical application of the interaction between light and a fluorescent compound via combining topical eosin and white light to treat skin tumors.[14-15] Since then, photodynamic therapy has progressed greatly and drastically over the years. Thomas J. Dougherty and co-workers through purifying a commercially available hematoporphyrin derivative were able produce the photosensitizer, Photofrin, in which in 1995 was approved by the US Food and Drug Administration (FDA) for cancer treatment.[13,16] Current research in this field is looking to broaden photodynamic therapy ability to treat all sorts of cancers as well as developing photosensitizers that are more powerful, more selective towards cancer cells and less toxic.[12]

1.6 Gasotransmitters

A new and blooming field within cancer treatment is the introduction of gasotransmitters. The terminology ‘gasotransmitters’ was first introduced in 2002 by Dr. Wang from the University of Saskatchewan to characterize molecules such as hydrogen sulfide (H_2S), carbon monoxide (CO) and nitric oxide (NO). So far, only these three molecules satisfy the proposed criteria to be classified as a gasotransmitter which includes: 1) They are small molecules of gas 2) They are freely permeable to membrane 3) They are endogenously and enzymatically generated and their generation is regulated 4) They have well-defined specific functions at physiologically relevant concentrations 5) Their cellular effects may or may not be mediated by second messengers, but should have specific cellular and molecular targets.[17] From this point on, CO will be the focal point

for gasotransmitters being discussed as studies revolving around CORMs (CO-releasing molecules) have been a major contributor to the present advancement of cancer treatment.

1.7 CO-Releasing Molecules

The use of CO within cancer treatment has been a growing subject for the biggest part of the past two decades. The reason for this growth is due to the ability for CO to overcome drug resistance amongst the cancer cells.[18] The process in which this inhibition of drug resistance occurs is via CO's effect on the mitochondria of cells. In the presence of CO, interference with the cytochrome C oxidase enzyme occurs which results in disturbance of the oxidative phosphorylation process, thus hindering the production of energy by the mitochondria. Thereby, promoting mitochondrial exhaustion and hurting cell growth and proliferation amongst these targeted cells.[19]

It was originally assumed that the application of CO would be primarily through inhalation as the main route of administration. In this case the dose of CO is controlled through changing the concentration of CO and monitoring CO levels by measuring CO-Hb in the blood of the patient. However, the development of CO-releasing molecules (CORMs) has provided an alternative route to administering controlled amounts of CO for medical application. Opposed to inhaling gaseous CO, CORMs can deliver CO to biological systems via injection into the systemic circulation while also limiting CO-Hb buildup.[19]

Motterlini and Foresti are scientists who are considered to pioneer some of the first CORMs to be developed, which includes Mn_2CO_{10} (CORM-1), tricarbonyldichlororuthenium-(II)-dimer (CORM-2) and tricarbonylchloro(glycinato)-

ruthenium (II) (CORM-3). [20-21] These CORMs are what would be considered metal-based CORMs and despite being categorized in the same group, they all pose quite different properties which make them unique. For example, the mode of release for CO is induced by light for CORM-1, whereas CORM-2 is observed to undergo ligand substitution in the presence of DMSO to afford the release of CO. While both of these CORMs require ethanol and DMSO to solubilize, CORM-3, on the other hand, is soluble in water. CORM-3 is a derivative of CORM-2 in which the monomer unit of CORM-2 is coordinated to glycine which allows for the aqueous solubility of the compound. Release of CO from CORM-3 is observed through ligand substitution as well when under physiological conditions.[20] One main limitation of these metal-based CORMs is the inherent cytotoxicity due to the metal atom, thus advancements to improve this limitation has led to the birth of new breeds of CORMs including enzyme-activated CORMs (ET-CORMs), photo-activated CORMs (PHOTO-CORMs) and bifunctional hybrid molecules (i.e., CORMs conjugated to nanoparticles and biological scaffolds).[22-24]

1.8 Purpose

The purpose of this research is to further improve this strategy of CO delivery using CORMs which possess favorable characteristics such as water-solubility, low-cytotoxicity and the ability to control the quantity of CO being released. Our group has successfully synthesized a PHOTO-CORM, known as bis-(2-hydroxynaphth-1-yl)cyclopropenone (DHNCP), which check marks all those boxes by being metal-free organic compound which uses UV and visible light as a source of irradiation to control the release of CO.

1.9 References

1. What is cancer? https://www.cancer.gov/about-cancer/understanding/what-is-cancer (accessed May 10, 2022).
2. Metastatic cancer: When cancer spreads. https://www.cancer.gov/types/metastatic-cancer#:~:text=moving%20through%20the%20walls%20of,tissue%20until%20a%20tiny%20tumor (accessed Jun 13, 2022).
3. Signs and symptoms of cancer. https://www.cancer.org/treatment/understanding-your-diagnosis/signs-and-symptoms-of-cancer.html (accessed Jun 13, 2022).
4. Arruebo, M.; Vilaboa, N.; Sáez-Gutierrez, B.; Lambea, J.; Tres, A.; Valladares, M.; González-Fernández, Á. Assessment of the Evolution of Cancer Treatment Therapies. *Cancers* **2011**, *3* (3), 3279–3330.
5. Arruda, W. O. Wilhelm Conrad Röntgen: 100 Years of X-Rays Discovery. *Arquivos de Neuro-Psiquiatria* **1996**, *54* (3), 525–531.
6. Taylor, A. Intensity-Modulated Radiotherapy - What Is It? *Cancer Imaging* **2004**, *4* (2), 68–73.
7. Computed Tomography (CT) SCAN. https://www.hopkinsmedicine.org/health/treatment-tests-and-therapies/computed-tomography-ct-scan#:~:text=A%20CT%20scan%20is%20a%20diagnostic%20imaging%20procedure%20that%20uses,detailed%20than%20standard%20X%2Drays (accessed Jun 14, 2022).
8. Chemotherapy to treat cancer. https://www.cancer.gov/about-cancer/treatment/types/chemotherapy (accessed Jun 16, 2022).
9. How chemotherapy works. https://www.cancerresearchuk.org/about-cancer/treatment/chemotherapy/how-chemotherapy-works#:~:text=Chemotherapy%20damages%20the%20genes%20inside,such%20as%20most%20normal%20cells (accessed Jun 16, 2022).
10. Radiation therapy for cancer. https://www.cancer.gov/about-cancer/treatment/types/radiation-therapy (accessed Jun 16, 2022).
11. The science behind Radiation therapy - american cancer society. https://www.cancer.org/content/dam/CRC/PDF/Public/6151.00.pdf (accessed Jun 16, 2022).
12. Photodynamic therapy to treat cancer. https://www.cancer.gov/about-cancer/treatment/types/photodynamic-therapy (accessed Jun 16, 2022).
13. Correia, J. H.; Rodrigues, J. A.; Pimenta, S.; Dong, T.; Yang, Z. Photodynamic Therapy Review: Principles, Photosensitizers, Applications, and Future Directions. *Pharmaceutics* **2021**, *13* (9), 1332.
14. Ackroyd, R.; Kelty, C.; Brown, N.; Reed, M. The History of Photodetection and Photodynamic Therapy. *Photochemistry and Photobiology* **2001**, *74* (5), 656.
15. Tappeiner, H. von; Jesionek, A. Therapeutische Versuche mit fluoreszierenden Stoffen. *Muench. Med. Wochenschr* **1903**, *50, 2042-2044*

16. Dougherty, T. J.; Gomer, C. J.; Henderson, B. W.; Jori, G.; Kessel, D.; Korbelik, M.; Moan, J.; Peng, Q. Photodynamic Therapy. *JNCI Journal of the National Cancer Institute* **1998**, *90* (12), 889–905.
17. Wang, R. Two's Company, Three's A Crowd: Can H2s Be the Third Endogenous Gaseous Transmitter? *The FASEB Journal* **2002**, *16* (13), 1792–1798.
18. Cui, Q.; Liang, X.-L.; Wang, J.-Q.; Zhang, J.-Y.; Chen, Z.-S. Therapeutic Implication of Carbon Monoxide in Drug Resistant Cancers. *Biochemical Pharmacology* **2022**, *201*, 115061.
19. Motterlini, R.; Otterbein, L. E. The Therapeutic Potential of Carbon Monoxide. *Nature Reviews Drug Discovery* **2010**, *9* (9), 728–743.
20. Ryter, S. W.; Ma, K. C.; Choi, A. M. Carbon Monoxide in Lung Cell Physiology and Disease. *American Journal of Physiology-Cell Physiology* **2018**, *314* (2).
21. Ji, X.; Damera, K.; Zheng, Y.; Yu, B.; Otterbein, L. E.; Wang, B. Toward Carbon Monoxide–Based Therapeutics: Critical Drug Delivery and Developability Issues. *Journal of Pharmaceutical Sciences* **2016**, *105* (2), 406–416.
22. Clark, J. E.; Naughton, P.; Shurey, S.; Green, C. J.; Johnson, T. R.; Mann, B. E.; Foresti, R.; Motterlini, R. Cardioprotective Actions by a Water-Soluble Carbon Monoxide–Releasing Molecule. *Circulation Research* **2003**, *93* (2).
23. Stamellou, E.; Storz, D.; Botov, S.; Ntasis, E.; Wedel, J.; Sollazzo, S.; Krämer, B. K.; van Son, W.; Seelen, M.; Schmalz, H. G.; Schmidt, A.; Hafner, M.; Yard, B. A. Different Design of Enzyme-Triggered Co-Releasing Molecules (ET-Corms) Reveals Quantitative Differences in Biological Activities in Terms of Toxicity and Inflammation. *Redox Biology* **2014**, *2*, 739–748.
24. Pai, S.; Hafftlang, M.; Atongo, G.; Nagel, C.; Niesel, J.; Botov, S.; Schmalz, H.-G.; Yard, B.; Schatzschneider, U. New Modular Manganese(I) Tricarbonyl Complexes as PhotoCORMs: In Vitro Detection of Photoinduced Carbon Monoxide Release Using COP-1 as a Fluorogenic Switch-on Probe. *Dalton Transactions* **2014**, *43* (23), 8664.

CHAPTER 2

Quantification of Bis-(2-hydroxynaphth-1-yl)cyclopropenone

2.1 Synthesis of DHNCP

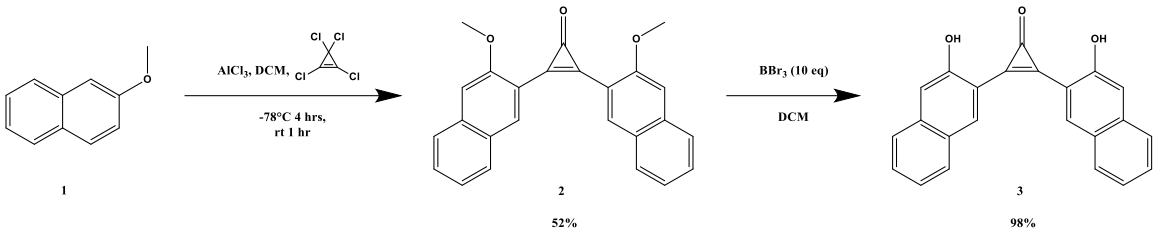

Scheme 2.1. Synthesis of Bis-(2-hydroxynaphth-1-yl)cyclopropenone

The synthesis of DHNCP as shown in **Scheme 2.1** starts with commercially purchased 2-methoxynaphthalene undergoing a Friedel-Crafts reaction with tetrachlorocyclopropenone to afford bis-(2-methoxybaphth-1-yl)cyclopropenone (DMNCP). The compound is then reacted with 10 equivalents of BBr_3 to perform demethylation of the methoxy groups into hydroxy functional groups, thus affording DHNCP as the final product. **Scheme 2.2** shows the release of CO from the cyclopropenone ring when exposed to a suitable light source which produces bis-(2-hydroxynaphth-1-yl)acetylene (DHNA).

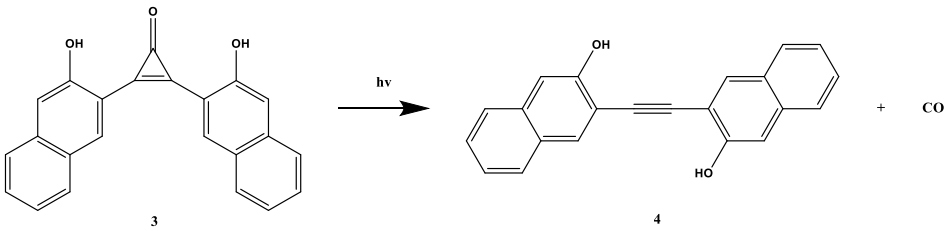

Scheme 2.2 Release of CO from DHNCP upon exposure to light

2.2 Aqueous Solubility

With the expectation of DHNCP to be applicable for in vivo and in vitro studies, it is important to understand the aqueous solubility of the compound as it will need to be compatible within physiological conditions.

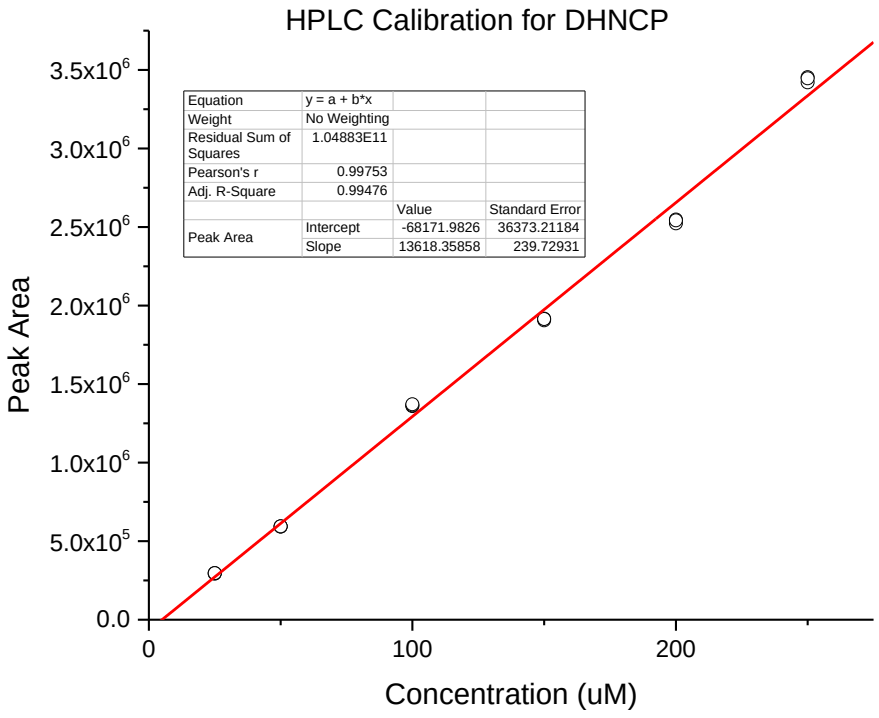

Figure 2.1. Peak area vs. concentration (μM) of DHNCP in methanol for samples of the following concentrations: 25 μM, 50 μM, 100 μM, 150 μM, 200 μM and 250 μM.

Using the linear regression equation obtained from **Figure 2.1**, the following steps are used to calculate the aqueous solubility:

$$y = (1.36 * 10^{10})x - (7 * 10^{4})\frac{mau}{min}$$

where x = the concentration of DHNCP (M) and y = the peak area (mau/min).

The peak area of the saturated DHNCP in biphosphate buffer obtained from **Figures 2.8** can then be substituted into the equation (1):

$$x = [DHNCP] = \frac{(1.45 * 10^6 + 7 * 10^4)}{1.36 * 10^{10}} = (1.1 \pm 0.005) * 10^{-4}\ M\ or\ 110 \pm 0.5\ \mu M$$

Resulting in a value of 110 ± 0.5 μM for the aqueous solubility of DHNCP. The following experiments such as quantum yield determination, pKa determination and CO quantification can now be tailored towards this newfound solubility of the compound.

2.3 pKa Determination

Due to both DHNCP and DHNA containing two hydroxy groups, it is important to understand how acidic and basic environments would affect the ionization of these compounds and this information can allow for the calculation of the pKa(s).

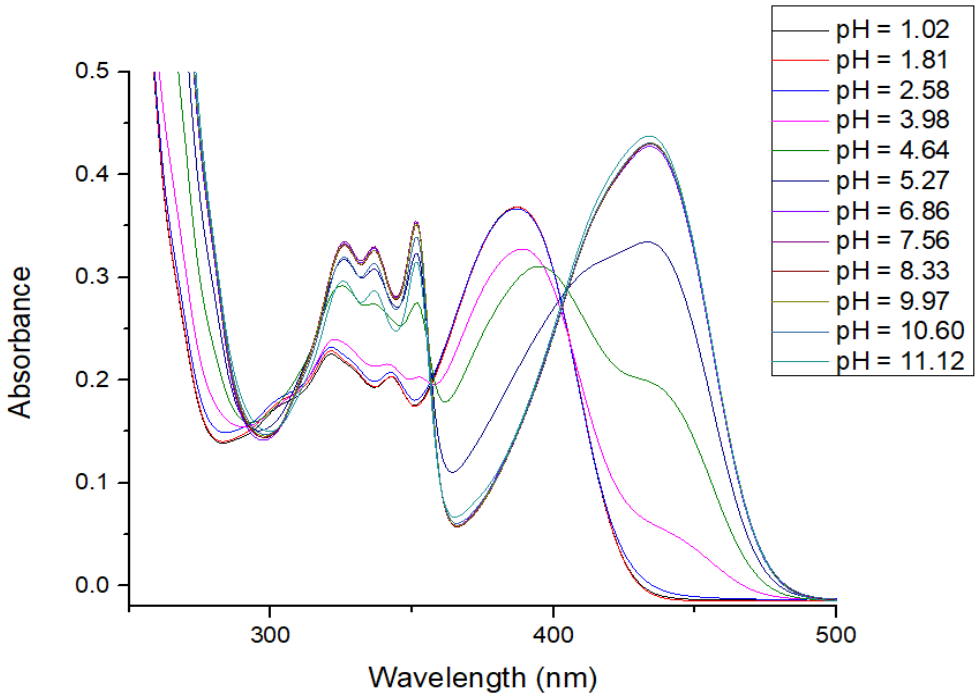

Figure 2.2. Absorbance vs Wavelength spectra of 50 μM DHNCP in various buffer solutions ranging from pH = 1.02 to pH = 11.12.

Figure 2.2 shows the evolution of the UV-Vis spectrum of DHNCP when measured in a set of solutions with pH values ranging from 1.02 to 11. 12. There is a clear bathochromic shift occurring for the absorption peak at ~380 nm for DHNCP in an acidic environment which can be seen at ~430 nm when in a basic environment. This change indicates that the molecule is experiencing some structural change which can be pointed towards one of the hydroxy groups being ionized under basic conditions.

To determine pKa, at various wavelengths, absorbance was plotted against pH to produce a scatter plot in which the following equation was used to fit the data to solve for K_a:

$$A_t = \frac{([H^+] * A_0 + A_e * K_a)}{([H^+] + K_a)}$$

where A_t = total absorbance of the sample at desired λ, A_o = absorbance of sample when pH << pKa, A_e = absorbance of sample when pH >> pKa.

Using this equation as the fitting equation for this relationship, the K_a value can be determined. The last step is substituting this value into the following equation to obtain the pKa:

$$pKa = -log_{10}(K_a)$$

Conducting this process over the wavelengths of 360, 380 and 420 nm, the resulting pKa for DHNCP is calculated to be 4.7 ± 0.1. As mentioned previously, it is expected that

there are multiple forms of DHNCP. Inputting the absorbance versus wavelength data collected into Origin and running a global fit which allows for the calculation of pKa over a range of wavelengths instead of a single wavelength, a pKa value of 3.4 ± 0.4 was calculated. Thus, $pKa_1 = 3.4 \pm 0.4$ and $pKa_2 = 4.7 \pm 0.1$ for DHNCP.

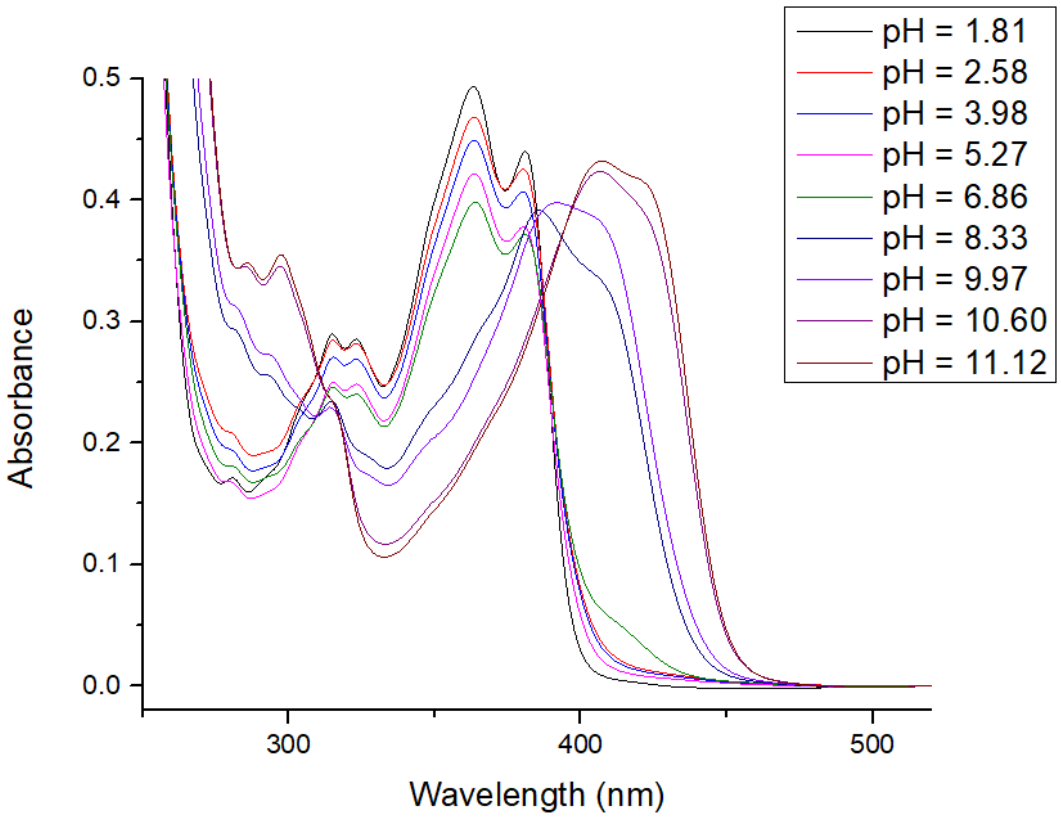

Figure 2.3. Absorbance vs Wavelength spectra of 50 μM DHNA in various buffer solutions ranging from pH = 1.81 to pH = 11.12.

Figure 2.3 shows the evolution of the UV-Vis spectrum of DHNA when measured in a basic, neutral, and acidic environment. Similarly, to DHNCP, the same steps were repeated at wavelengths 325 nm, 350 nm, 364 nm, 410 nm and 420 nm to determine pKa. The pKa was calculated to be 7.31 ± 0.04. Again, a global fitting is used to determine the other possible pKas. The second value obtained from this process was 9.4 ± 0.1. Thus, $pKa_1 = 7.31 \pm 0.04$ and $pKa_2 = 9.4 \pm 0.1$ for DHNA.

2.4 Quantum Yield

Given that a major characteristic of DHNCP is the ability to control CO release with duration or intensity of irradiation, quantum yield is an extremely important piece of information to measure for the compound as it provides further understanding of the photochemical release of CO. The following equation was used to calculate the quantum yield of the substrate:

$$\Phi_s = \frac{k_s \Phi_a (1 - 10^{-Abs(a)})}{k_a (1 - 10^{-Abs(s)})}$$

Where Φ_a and k_a represents the quantum yield and rate of conversion, respectively, of the chemical actinometer and Φ_s and k_s represents the quantum yield and rate of conversion of the substrate.

Solvent	Φ (λ = 350 nm)	Φ (λ = 420 nm)
MeOH	N/A	0.243 ± 0.0008
DCM	N/A	0.0976 ± 0.002
Biphosphate Buffer	0.0048 ± 0.0002	0.0028 ± 0.0002

Table 2.1 Quantum yield values for DHNCP in solvents such as MeOH, DCM and Biphosphate buffer at λ = 350 and 420 nm.

The quantum yield for CO release using 420 nm light shows the highest value in MeOH at Φ_{420} = 0.243 ± 0.0008, followed by DCM with a value of Φ_{420} = 0.0976 ± 0.002 and biphosphate buffer with a much lower value at Φ_{420} = 0.0028 ± 0.0002. It is to be noted that the quantum yield values for the trials in MeOH and DCM were obtained using only a single 420 nm lamp wrapped in mostly black aluminum foil to control the intensity of light exposure as opposed to using 2 420 nm lamps for the biphosphate buffer trial. To ensure increased accuracy in calculating quantum yield, ~ 10% conversion of the substrate must be observed after a minimum of 60 seconds of irradiation. In this case,

wrapping the lamps in foil aimed to decrease the energy output of light to allow for slower conversion of the substrate as previous trials have seen greater than 10% conversion in under 60 seconds of irradiation using a fully uncovered 420 nm lamp. After the wavelength of light from 420 nm to 350 nm, the quantum yield for DHNCP in the biphosphate buffer solution increased to a value of $\Phi_{350} = 0.0048 \pm 0.0002$. This proves that increasing the energy of light by decreasing the wavelength correlates to an increase in CO release. Overall, the ability to induce the release of CO when subjected to visible light is a very promising characteristic, especially with the goal of implementing this process in a medical environment to aid in the alleviation of cancerous cells.

2.5 Fluorescence Quantum Yield

The following equation was used to calculate the fluorescence quantum yield of the substrate:

$$\phi_X = \phi_{ST}\left(\frac{I_x}{I_{ST}}\right)\left(\frac{1-10^{-Abs_{ST}}}{1-10^{-Abs_X}}\right)\left(\frac{\eta_X}{\eta_{ST}}\right)^2$$

By plotting Intensity area vs $1\text{-}10^{-Abs}$, where absorbance is the absorbance value at the excitation wavelength for the compound, the Grad value is determined via the slope of the graph thus allowing for the equation to simplify to:

$$\phi_X = \phi_{ST}\left(\frac{Grad_X}{Grad_{ST}}\right)\left(\frac{\eta_X}{\eta_{ST}}\right)^2$$

Where ‘X’ represents the sample and ‘ST’ represents the actinometer. Grad refers to the slope of intensity area vs absorbance and η represents the refractive index of the solvent.

η_X = 1.333 (this value is the same for both the phosphate buffer and HCl samples) and η_{ST} = 1.3614. The fluorescence quantum yield of the actinometer (φ_{ST}) = 0.73 ± 0.094.

	Quantum Yield (φ_X)	
Trial	Biphosphate Buffer	0.001M HCl
1	0.056 ± 0.04	0.046 ± 0.03
2	0.048 ± 0.03	0.055 ± 0.03
3	0.053 ± 0.02	0.049 ± 0.03
Average	0.052 ± 0.03	0.050 ± 0.03

Table 2.2. Fluorescence quantum yield values for DHNA in biphosphate buffer and 0.001M HCl across three trials.

According to **Table 2.2**, the average fluorescent quantum yield for DHNA in biphosphate buffer is Φ = 0.052 ± 0.03 which is comparable average fluorescent quantum yield in 0.001 M HCl which calculated to Φ = 0.050 ± 0.03. Both values are very similar, which is a bit surprising. It was originally hypothesized that the quantum yield values for the DHNA in phosphate buffer to be a bit greater due to partial dissociation of hydrogen from the hydroxy group, as seen in the pKa determination, thus presenting an O^- group which is a very strong electron donating group and fluorescence shows a pattern of increasing intensity in the presence of EDGs. Nevertheless, the fluorescent properties of DHNA can allow for the ability to trace the release of CO from DHNCP through measuring the intensity of the emission.

2.6 CO Quantification

A myoglobin assay is used to track and measure the release of CO from DHNCP due to the high affinity of the heme group on myoglobin towards CO. As CO release is induced via light, a control experiment was first conducted to ensure that the absorbance spectrum of myoglobin is unaffected as there are mentions that myoglobin can decompose in the presence of strong UV light.

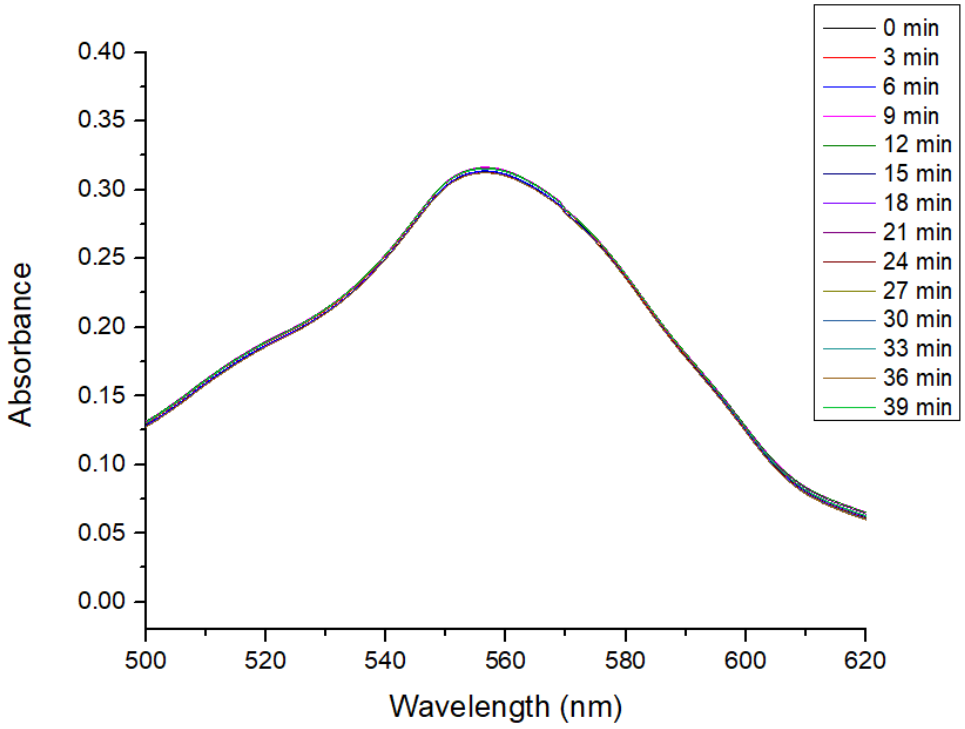

Figure 2.4. 32.2 μM deoxy-Mb solution irradiated using 4 350 nm lamps at 3-minute intervals for a total irradiation time of 39 minutes.

Figure 2.4 shows the absorbance spectrum of myoglobin as the solution is irradiated under 350 nm light. The original concerns of myoglobin decomposing can be nullified as there is no observable change in the spectral region of 500 – 600nm which is the range that will be used to calculate and observe the release of CO.

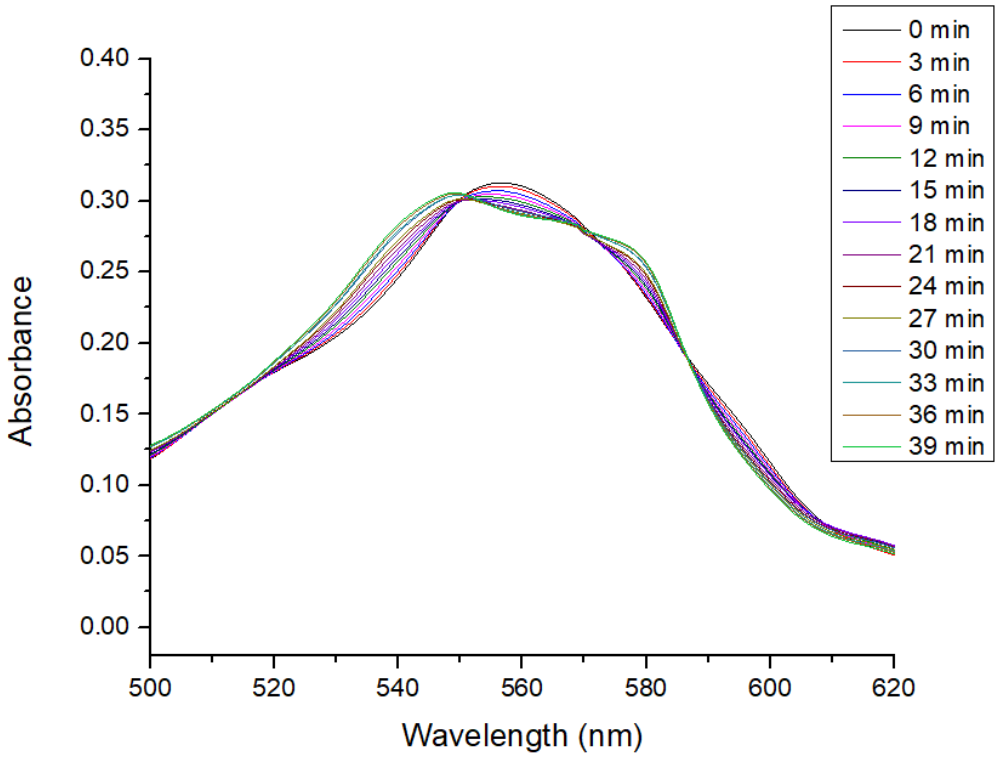

Figure 2.5. 20 μM DHNCP in Myoglobin irradiated using 4 350 nm lamps at 3-minute intervals for a total irradiation time of 39 minutes.

Figure 2.5 shows a clear evolution of the spectrum as the major peak for deoxy-Mb at λ = 557 nm transitions towards two new major absorbance peaks at λ = 540 and 587 nm being to emerge. These two peaks are representative peaks that CO-Mb is being formed while the decrease in absorbance for the peak at 557 nm indicated the decrease in concentration of deoxy-Mb within the solution. By taking the absorbance values at λ = 540 nm, the concentration of CO released can be calculated by using the following equation:

$$[CO] = \Delta[Mb] = \frac{\Delta Abs}{\Delta \varepsilon}$$

Where Δε represents the difference between the extinction coefficient for CO-Mb (ε = 15,400 $M^{-1}cm^{-1}$) and the extinction coefficient for deoxy-Mb (ε =7480 $M^{-1}cm^{-1}$) at λ = 540 nm.

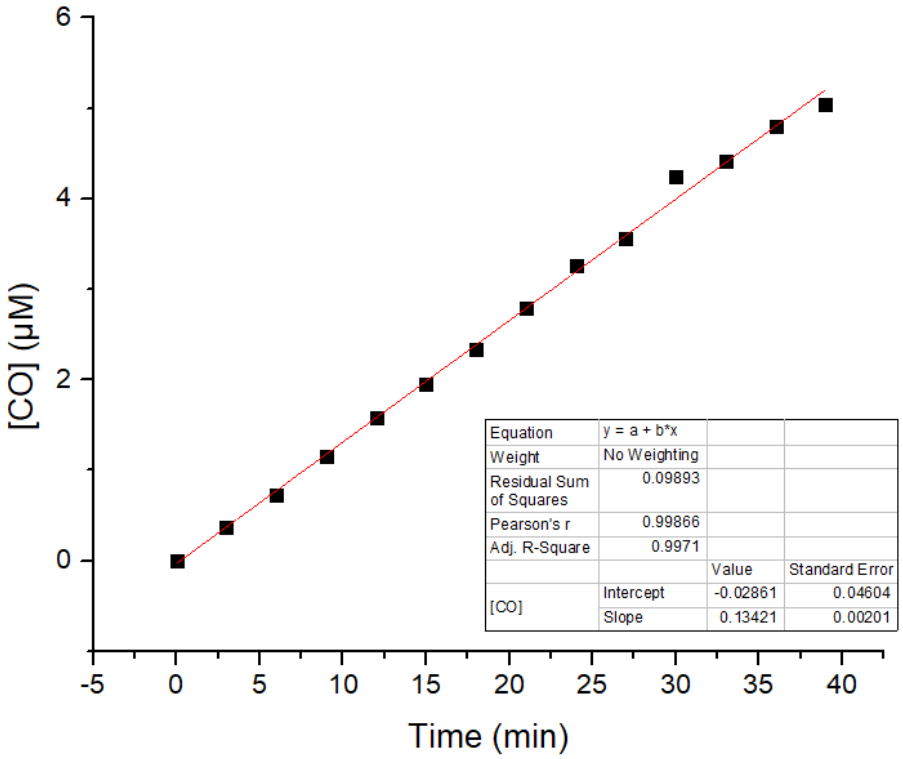

Figure 2.6. Concentration of CO release vs Time at λ = 540 nm for a sample of 20 μM DHNCP in Myoglobin after a total irradiation time of 39 minutes using 4 350 nm lamps.

Figure 2.6 shows a linear relationship between irradiation time and the amount of CO being released from DHNCP. The slope of this relationship is determined to be 0.134 μM of CO released per minute. After the total irradiation time of 39 minutes, 5.04 μM which is approximately a 25% conversion rate of DHNCP, given the molar ratio of DHNCP to CO is 1:1, to its acetylene counterpart. Thus, under the conditions of 4 350 nm lamps, it would take about 160 minutes to fully release 20 μM of CO. More importantly, this data portrays the defining characteristics of this compound in which the release of CO can be controlled via changes in irradiation time. The rate of release of CO can also be altered

by increasing or decreasing the wavelength of light used for irradiation. Although it would have been ideal in this experiment to show the release of CO when subjected to 420 nm light as previously shown in the quantum yield data, Myoglobin, unfortunately, shows an overwhelmingly strong absorbance band at 420 nm which would interfere with the photolysis of DHNCP.

2.7 Cell Viability

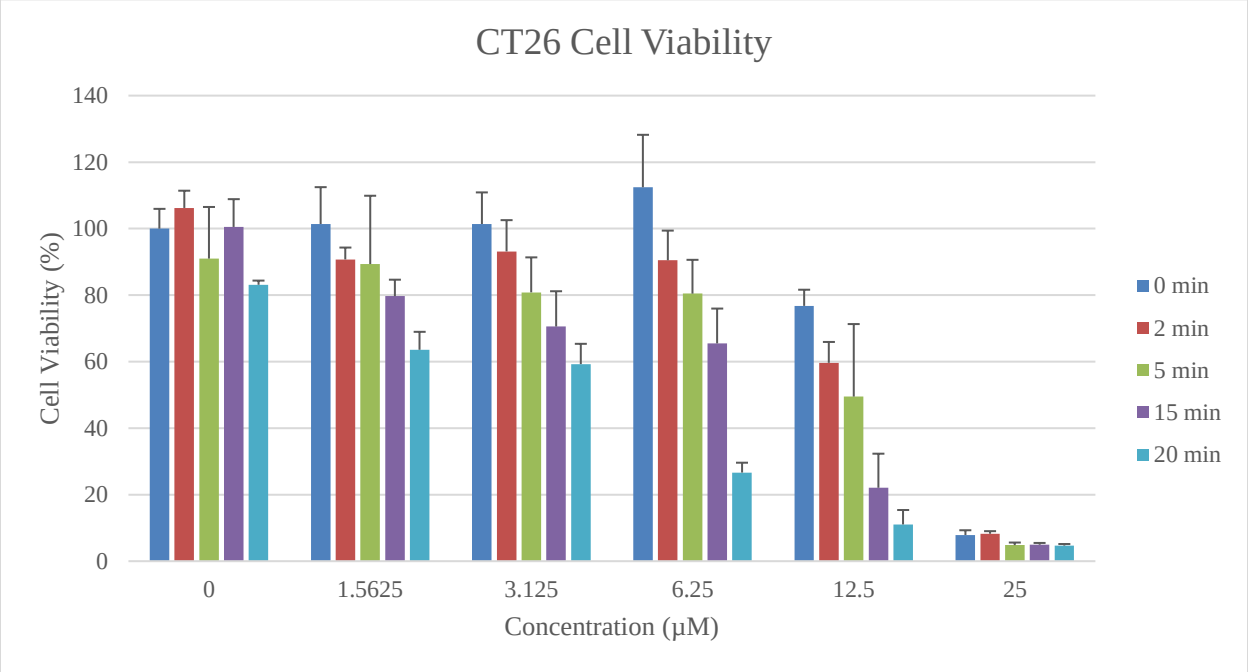

Figure 2.7. Cell viability for CT26 colon cancer cells in increasing concentrations of DHNCP with increasing exposure of 365 nm light.

Figure 2.7 shows the cell viability of a CT26 colon cancer cell line when subjected to varying concentrations of DHNCP and irradiation time using 365 nm light. It is observed that an increase in irradiation time and an increase in concentration of the CORM does reduce cell viability with longer exposure to light showing a greater decrease in the cell's viability as more CO can be released. Interestingly, when the concentration of the CORM

added exceeds 12.5 μM, the cancer cells show and initial decrease to ~80% viability without any light exposure and after 25 μM of CORM is added to the cells, the cell viability reduces drastically to less than 10% without any light irradiation. This indicates that DHNCP itself is toxic towards CT26 cells at concentrations of 12.5 μM and higher, however the explanation for this is currently unknown and requires further experiments to deduce the cause of such observation.

2.8 Experimental Section

Materials: All reagents were purchased from commercial suppliers and used as received unless otherwise noted.

Preparation of bis-(2-methoxynaphth-1-yl)cyclopropenone (DMNCP): A 250 mL round bottom flask is degassed at room temperature under nitrogen. Then 1.69 g (12.64 mmol) $AlCl_3$ and 100 mL of DCM are added to the round bottom flask and stirred for 5 minutes while under nitrogen. The remainder of this experiment will be conducted with the solution under Nitrogen. Using a micro-syringe, 0.776 mL (6.32 mmol) of tetrachlorocyclopropenone is added to the round bottom flask and stirred for an additional 10 minutes. The solution is transferred to a dry ice bath to stir for an additional 5 minutes. 2.00 g (12.64 mmol) of 2-methoxynaphthalene dissolved in ~ 10 mL DCM is then added slowly to the round bottom flask using a syringe over the course of ~ 10 minutes. The solution is then allowed to stir in the dry ice bath (dry ice in acetone) for 4 hours before being taken out of the dry ice bath to stir for an additional 1 hour. The round bottom flask is removed from the Nitrogen and then the solution is transferred to a 1000 mL separatory funnel to be quenched with ~ 80 mL 5% HCl. The organic layer is then washed with ~ 100 mL of Brine and then the organic layer is transferred to a 250 mL

Erlenmeyer flask. The solution is dried using Sodium Sulfate anhydrous and then transferred to a 500 mL round bottom flask to be placed on the Rotovap to distill the solvent. A mobile phase of 1:4 EtOAc/Hexane is used to purify the product spot (R_f = 0.67) via column chromatography. ^{1}H NMR: Varian 400, in CDCl3: ^{1}H-NMR (CDCl3), δ (ppm): 8.30-8.32 (d, 2H), 8.04-8.06 (d, 2H), 7.84-7.86 (d, 2H), 7.58-7.61 (2, 1H), 7.42-7.46 (t, 2H), 7.29-7.32 (d, 2H), 3.68 (s, 6H). ^{13}C NMR: Varian 400, in CDCl3: ^{13}C-NMR (CDCl3), δ (ppm): 158., 157.43, 145.76, 134.50, 133.73, 128.54, 128.30, 128.16, 125.59, 124.52, 112.33, 109.55, 55.97.

Preparation of bis-(2-hydroxynaphth-1-yl)cyclopropenone (DHNCP): In a 100 mL round bottom flask, 1.20 g (3.27 mmol) of DMNCP is dissolved in 40 mL DCM under nitrogen. The flask is then transferred to a dry ice bath and stir for 10 minutes. 3.10 mL (32.7 mmol) of BBr3 is then slowly added to the round bottom flask using a micro-syringe while still under nitrogen. The solution is allowed to stir for 4 hours and then the flask is removed from the dry ice bath to continue stirring overnight at room temperature. The flask is then placed in an ice bath and stirred for 15 minutes. Remove the flask from being under nitrogen and then add ~ 15 mL of DI water dropwise to the flask until fuming stops. Rinse the sides of the flask with DCM and then stir for 30 minutes. Suction filtration is then performed on the solution. Cold DI water is used to rinse the round bottom flask to ensure all content is filtrated. While the sample is being filtrated, ~ 20 mL of DI Water is used to rinse the product to impurities. Additional DI Water can be used to continue rinsing the compound as needed until a dark yellow color is observed. Air is continued to be pulled through for an additional 30 minutes before disconnecting the vacuum and allowing the filtrate to dry overnight. ^{1}H NMR: Varian 400: 1H-NMR

(DMSO), δ (ppm): 10.78 (s, 2H), 8.10-8.12 (d, 2H), 8.02-8.04 (d, 2H), 7.89-7.91 (d, 2H), 7.55-7.59 (t, 2H), 7.38-7.42 (t, 2H), 7.25-7.27 (d, 2H). ^{13}C NMR: Varian 400: 13C-NMR (DMSO), δ (ppm): 157.14, 156.13, 144.80, 134.05, 133.30, 128.29, 127.74, 127.46, 124.18, 123.54, 118.23, 106.18.

Aqueous Solubility of DHNCP: A set of standards were prepared by a stock solution of 0.02M DHNCP in DMSO in Methanol to provide the following solutions: 25 µM, 50 µM, 100 µM, 150 µM, 200 µM and 250 µM. The following solutions were then analyzed via HPLC to obtain the peak area value for DHNCP. This was repeated in triplicate. Parameters for HPLC includes: 75% MeOH:H_2O for the solvent, 10 minute run time and the DHNCP peak of interest = ~ 5.3 min.

Each trial was then plotted in Origin to produce a Peak Area vs Concentration standard curve and then the slope-intercept equation was derived.

A known concentration of solid DHNCP was diluted in biphosphate buffer (IS = 0.1M, BR = 0.25, pH = 7.48) and sonicated for 1 hour to produce a DHNCP in BP solution. Two 2 mL Eppendorf tubes were then filled with 1 mL of the resulting solution and then centrifuged for 15 minutes at 15000 RPM. After the initial centrifuge, the supernatant was then transferred to two more 2 mL Eppendorf tubes, this time filled to only 0.5 mL per tube, and centrifuged again for 15 minutes at 15000 RPM to ensure all solid particles are fully separated from the liquid solution. Lastly, the final supernatant was then analyzed via HPLC via the same parameter from above. This was repeated in triplicate.

The resulting peak area from the BP samples were then substituted into the respective derived slope-intercept equations from the standards to yield the

concentration of the DHNCP. This value indicates the maximum solubility of DHNCP in BP.

pKa determination of DHNCP: A set of buffers were produced ranging from pH = 1.02 to pH = 11.12 using the following reagents: perchloric acid ($HClO_4$), acetic acid, monobasic sodium phosphate anhydrous, dibasic sodium phosphate anhydrous and tribasic sodium phosphate anhydrous. Samples were prepared in a quartz cuvette by adding 0.3 mL of 500 μM DHNCP in DMSO stock solution to 2.7 mL buffer solution. 50 μL of MeOH was used as a co-solvent to ensure that DHNCP is fully dissolved in the buffer solutions. The Cary-5000 UV spectrophotometer was then used to obtain UV spectral data of each sample. Each sample had a baseline taken of their respective solvent before UV analysis was conducted.

A set of buffers were produced ranging from pH = 1.81 to pH = 11.12. Samples were prepared in a quartz cuvette by adding 0.3 mL of 500 μM DHNA in DMSO stock solution to 2.7 mL buffer solution. No co-solvent was used for these samples as precipitation was observed when MeOH was added to various buffer samples. The Cary-5000 UV spectrophotometer was then used to obtain UV spectral data of each sample. Each sample had a baseline taken of their respective solvent before UV analysis was conducted.

Quantum Yield Determination: 350 nm: A solution of 0.136 mM 4-NV was produced by dissolving 0.0025 grams (.0136 mmol) in 100 mL of 0.5M KOH. An initial absorbance spectrum of the solution was then recorded using the Cary-5000 UV Spectrophotometer. A 2.5 - 3 mL aliquot of the 4-NV solution was injected into a quartz cuvette and its initial absorbance spectrum was observed. The sample was then irradiated

under 2 350 nm lamps using a Rayonet for 15 seconds and then the absorbance spectrum of the samples was recorded again. This was repeated until a total irradiation of 60 seconds was achieved.

A sample of 100 µM of DHNCP in Phosphate buffer was produced by mixing 4 µL DHNCP in 4 mL of phosphate buffer solution. The sample was then transferred to a quartz cuvette and an initial absorbance spectrum was taken using the Cary 5000 UV-Spectrophotometer. The sample was then irradiated using a Rayonet with 2 350 nm lamps for a total irradiation time of 30-35 minutes until ~10% conversion was observed. UV spectra were taken of the sample at constant intervals throughout the irradiation of the sample. This was repeated for two more trials.

420 nm: A solution of 0.136 mM 4-NV in KOH was measured using the Cary-5000 UV Spectrophotometer to obtain the rate of conversion of the sample as it is subjected to irradiation over time. The sample was irradiated using one 420 nm lamp covered in black aluminum foil with a slit over a total irradiation time of 45 sec and another sample was irradiated using 4 420 nm lamps while observing the UV spectra every 15 sec.

A set of DHNCP samples MeOH and DCM were prepared in triplicates. The MeOH sample was prepared by adding 5 µL of DHNCP stock solution to 4 mL of MeOH to produce a 125 µM DHNCP in MeOH solution. The DCM sample was prepared by adding 5 µL of DHNCP stock solution to 4 mL of DCM to produce a 125 µM DHNCP in DCM solution. The MeOH and DCM samples were irradiated using one 420 nm lamps covered in black aluminum foil with a slit in the large Rayonet for a total irradiation time

of 8 min to obtain a conversion of ≤ 10%. The UV spectra of the samples were also taken throughout this time at varying intervals.

Fluorescence Quantum Yield Determination: A stock solution of the actinometer is prepared by dissolving 3.7 mg (0.016 mmol) Coumarin 460 in 80 mL of Ethanol to produce a ~0.2 mM solution. A set of samples were prepared by diluting 0.2 mM Coumarin in Ethanol stock solution to produce samples with concentrations of 1.5 μM, 2 μM, 2.5 μM, 3 μM and 3.5 μM. These concentrations were chosen as they are within the absorbance value constraint of ≤ ~ 0.05. The absorbance values of each sample were taken using the Cary-5000. The excitation wavelength of the sample can then be determined via the wavelength of max absorbance. The excitation wavelength (λ_{ex}) is determined to be 373 nm.

A set of DHNA in biphosphate buffer samples were prepared by diluting a 500 μM stock solution of DHNA in DMSO in biphosphate buffer to produce samples with concentrations of 5 μM, 6 μM, 7 μM, 8 μM and 9 μM. 50 μM of Methanol was used as a co-solvent to ensure that DHNA is fully dissolved. These concentrations were chosen as they are within the absorbance value constraint of ≤ ~ 0.05. The absorbance values of each sample were taken using the Cary-5000. The excitation wavelength of the same can then be determined via the wavelength of max absorbance. However, for these samples, the excitation wavelength was determined to be 363 nm which is not the wavelength of max absorbance, but it provides a larger area of intensity via the fluorescence data and considers the peak at 382 nm which is the wavelength of max absorbance.

A set of DHNA in HCl samples were prepared by diluting a 500 μM stock solution of DHNA in DMSO in 0.001 M HCl to produce samples with concentrations of

5 μM, 5.5 μM, 6 μM, 6.5 μM and 7 μM. These concentrations were chosen as they are within the absorbance value constraint of ≤ ~ 0.05. The absorbance values of each sample were taken using the Cary-5000. The excitation wavelength of the sample can then be determined via the wavelength of max absorbance. The excitation wavelength (λ_{ex}) is determined to be 362 nm.

CO Quantification: A 32 μM stock solution of Myoglobin is prepared by dissolving 32.2 mg (0.0019 mmol) of Myoglobin from equine skeletal muscle in 60 mL of biphosphate buffer (IS = 0.1 M, BR = 0.25, [H2PO4-] = 0.00625 M). In a glass vial, 3 mL of the Mb solution is reduced using sodium dithionite to create a 0.5% sodium dithionite solution. The newly prepared deoxy-Mb solution is then transferred into a quartz cuvette and 3 μL of 0.02M DHNCP in DMSO is added to the cuvette. Irradiation using 4 350 nm lamps in a Rayonet and UV-Vis analysis performed using a Cary-5000 Spectrophotometer is used to measure the release of CO.

MTT Analysis: CT26 cells were seeded at 8000 cells/well in a 96-well black plate overnight. DHNCP was then diluted with cell culture medium (RPMI-1640 + 10% FBS + 1% Pen Strep) and added to cells at concentrations 25, 12.5, 6.25, 3.125, and 1.5625 μM. The cell medium without DHNCP was used as a control. After adding the CORM to the solution, UV was irradiated on the cells for 0, 2, 5, 15 and 20 min, respectively. The cells were co-cultured with the CORM solution for 24 h. The CORM solution was then removed followed by adding MTT solution. After 4 h incubation, the supernatant was removed and DMSO was added to dissolve crystals. The absorbance value was measured by a plate reader at 570 nm.

2.9 References

1. What is cancer? https://www.cancer.gov/about-cancer/understanding/what-is-cancer (accessed May 10, 2022).
2. Metastatic cancer: When cancer spreads. https://www.cancer.gov/types/metastatic-cancer#:~:text=moving%20through%20the%20walls%20of,tissue%20until%20a%20tiny%20tumor (accessed Jun 13, 2022).
3. Signs and symptoms of cancer. https://www.cancer.org/treatment/understanding-your-diagnosis/signs-and-symptoms-of-cancer.html (accessed Jun 13, 2022).
4. Arruebo, M.; Vilaboa, N.; Sáez-Gutierrez, B.; Lambea, J.; Tres, A.; Valladares, M.; González-Fernández, Á. Assessment of the Evolution of Cancer Treatment Therapies. *Cancers* **2011**, *3* (3), 3279–3330.
5. Arruda, W. O. Wilhelm Conrad Röntgen: 100 Years of X-Rays Discovery. *Arquivos de Neuro-Psiquiatria* **1996**, *54* (3), 525–531.
6. Taylor, A. Intensity-Modulated Radiotherapy - What Is It? *Cancer Imaging* **2004**, *4* (2), 68–73.
7. Computed Tomography (CT) SCAN. https://www.hopkinsmedicine.org/health/treatment-tests-and-therapies/computed-tomography-ct-scan#:~:text=A%20CT%20scan%20is%20a%20diagnostic%20imaging%20procedure%20that%20uses,detailed%20than%20standard%20X%2Drays (accessed Jun 14, 2022).
8. Chemotherapy to treat cancer. https://www.cancer.gov/about-cancer/treatment/types/chemotherapy (accessed Jun 16, 2022).
9. How chemotherapy works. https://www.cancerresearchuk.org/about-cancer/treatment/chemotherapy/how-chemotherapy-works#:~:text=Chemotherapy%20damages%20the%20genes%20inside,such%20as%20most%20normal%20cells (accessed Jun 16, 2022).
10. Radiation therapy for cancer. https://www.cancer.gov/about-cancer/treatment/types/radiation-therapy (accessed Jun 16, 2022).
11. The science behind Radiation therapy - american cancer society. https://www.cancer.org/content/dam/CRC/PDF/Public/6151.00.pdf (accessed Jun 16, 2022).
12. Photodynamic therapy to treat cancer. https://www.cancer.gov/about-cancer/treatment/types/photodynamic-therapy (accessed Jun 16, 2022).
13. Correia, J. H.; Rodrigues, J. A.; Pimenta, S.; Dong, T.; Yang, Z. Photodynamic Therapy Review: Principles, Photosensitizers, Applications, and Future Directions. *Pharmaceutics* **2021**, *13* (9), 1332.
14. Ackroyd, R.; Kelty, C.; Brown, N.; Reed, M. The History of Photodetection and Photodynamic Therapy. *Photochemistry and Photobiology* **2001**, *74* (5), 656.
15. Tappeiner, H. von; Jesionek, A. Therapeutische Versuche mit fluoreszierenden Stoffen. *Muench. Med. Wochenschr* **1903**, *50, 2042-2044*

16. Dougherty, T. J.; Gomer, C. J.; Henderson, B. W.; Jori, G.; Kessel, D.; Korbelik, M.; Moan, J.; Peng, Q. Photodynamic Therapy. *JNCI Journal of the National Cancer Institute* **1998**, *90* (12), 889–905.
17. Wang, R. Two's Company, Three's A Crowd: Can H2s Be the Third Endogenous Gaseous Transmitter? *The FASEB Journal* **2002**, *16* (13), 1792–1798.
18. Cui, Q.; Liang, X.-L.; Wang, J.-Q.; Zhang, J.-Y.; Chen, Z.-S. Therapeutic Implication of Carbon Monoxide in Drug Resistant Cancers. *Biochemical Pharmacology* **2022**, *201*, 115061.
19. Motterlini, R.; Otterbein, L. E. The Therapeutic Potential of Carbon Monoxide. *Nature Reviews Drug Discovery* **2010**, *9* (9), 728–743.
20. Ryter, S. W.; Ma, K. C.; Choi, A. M. Carbon Monoxide in Lung Cell Physiology and Disease. *American Journal of Physiology-Cell Physiology* **2018**, *314* (2).
21. Ji, X.; Damera, K.; Zheng, Y.; Yu, B.; Otterbein, L. E.; Wang, B. Toward Carbon Monoxide–Based Therapeutics: Critical Drug Delivery and Developability Issues. *Journal of Pharmaceutical Sciences* **2016**, *105* (2), 406–416.
22. Clark, J. E.; Naughton, P.; Shurey, S.; Green, C. J.; Johnson, T. R.; Mann, B. E.; Foresti, R.; Motterlini, R. Cardioprotective Actions by a Water-Soluble Carbon Monoxide–Releasing Molecule. *Circulation Research* **2003**, *93* (2).
23. Stamellou, E.; Storz, D.; Botov, S.; Ntasis, E.; Wedel, J.; Sollazzo, S.; Krämer, B. K.; van Son, W.; Seelen, M.; Schmalz, H. G.; Schmidt, A.; Hafner, M.; Yard, B. A. Different Design of Enzyme-Triggered Co-Releasing Molecules (ET-Corms) Reveals Quantitative Differences in Biological Activities in Terms of Toxicity and Inflammation. *Redox Biology* **2014**, *2*, 739–748.
24. Pai, S.; Hafftlang, M.; Atongo, G.; Nagel, C.; Niesel, J.; Botov, S.; Schmalz, H.-G.; Yard, B.; Schatzschneider, U. New Modular Manganese(I) Tricarbonyl Complexes as PhotoCORMs: In Vitro Detection of Photoinduced Carbon Monoxide Release Using COP-1 as a Fluorogenic Switch-on Probe. *Dalton Transactions* **2014**, *43* (23), 8664.

LIST OF FIGURES

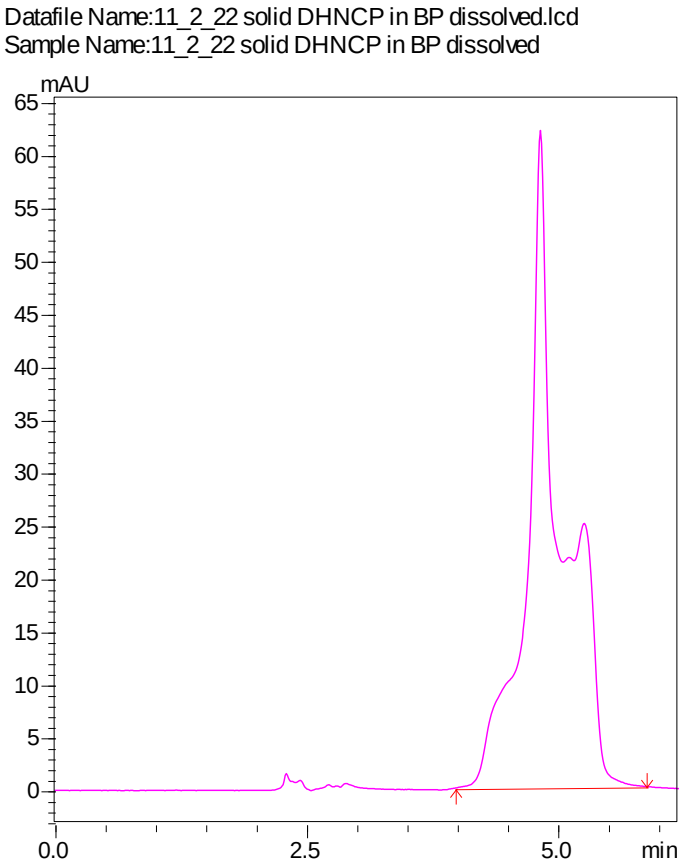

Figure 2.8. HPLC plot for a saturated solution of DHNCP dissolved in biphosphate buffer. Retention time = 5.3 minutes for DHNCP.

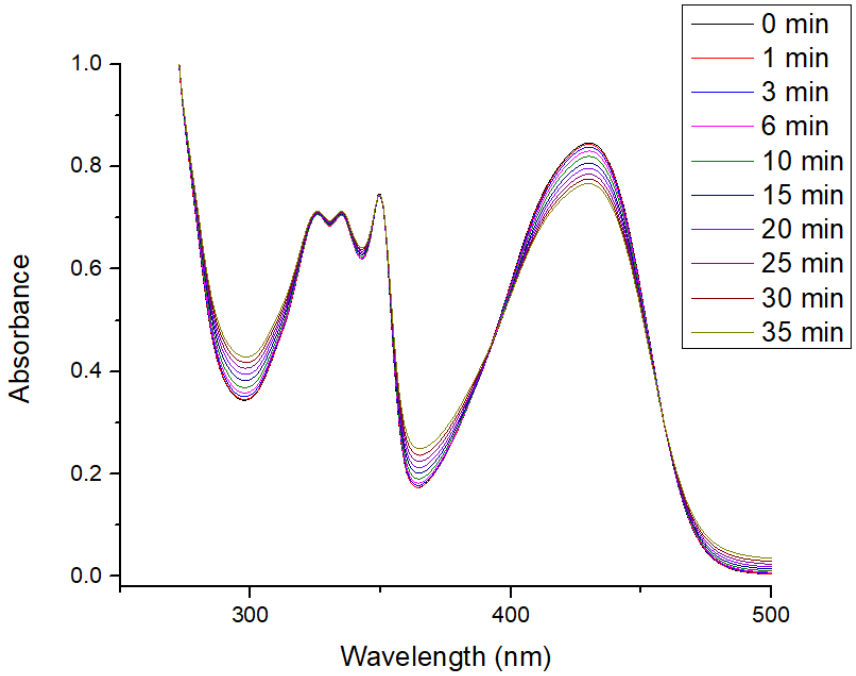

Figure 2.9. Absorbance vs Wavelength for a sample of 100 μM DHNCP in biphosphate buffer, irradiated using 2 350 nm lamps in a Rayonet.

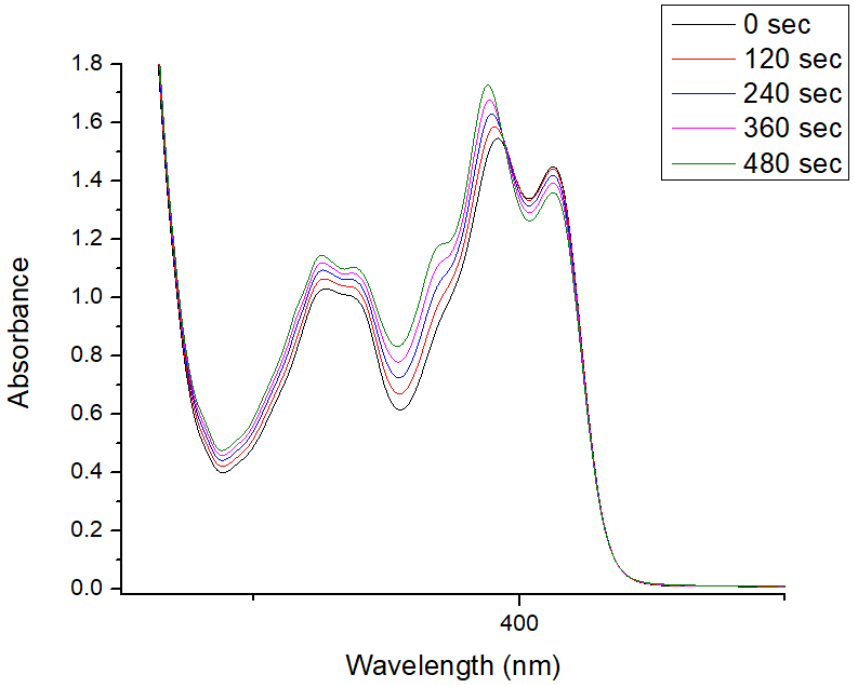

Figure 2.10. Absorbance vs Wavelength for a sample of 125 μM DHNCP in DCM irradiated using one 420 nm lamp covered in black aluminum foil in a Rayonet.

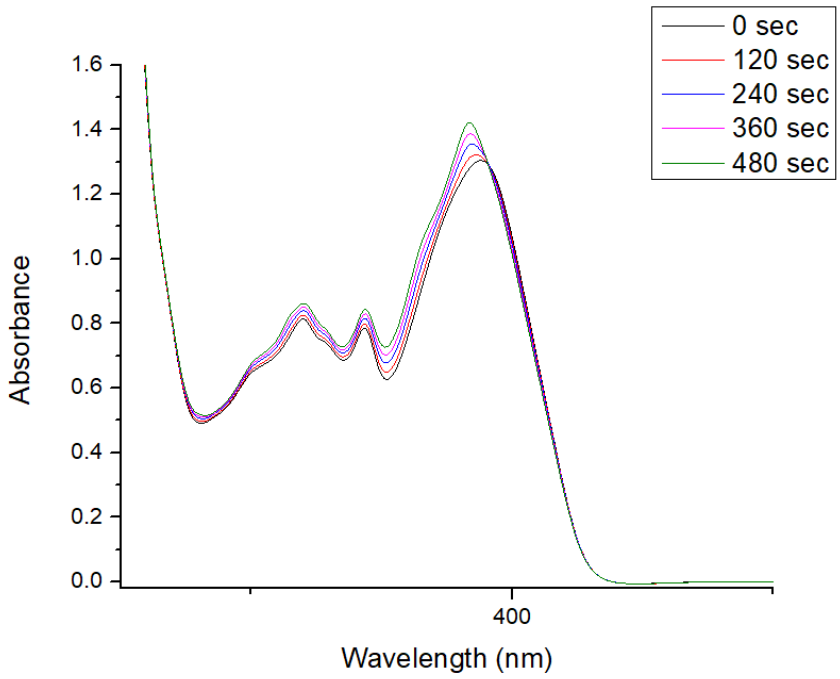

Figure 2.11. Absorbance vs Wavelength for a sample of 125 μM DHNCP in MeOH irradiated using one 420 nm lamp covered in black aluminum foil in a Rayonet.

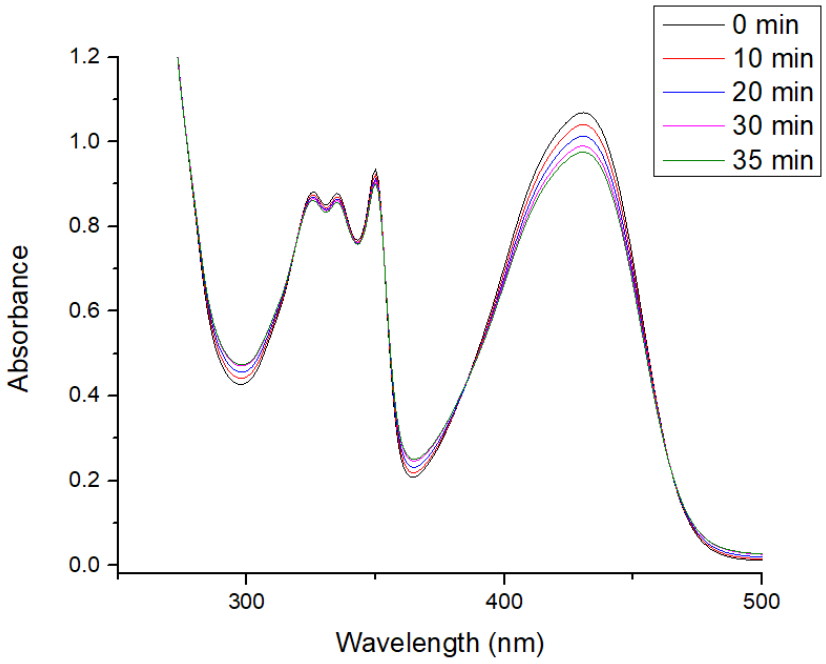

Figure 2.12. Absorbance vs Wavelength for a sample of 110 μM DHNCP in MeOH irradiated using 4 420 nm lamps in a Rayonet.